JOC The Journal of Organic Chemistry

ARTICLE

pubs.acs.org/joc

Rearrangement of 3-Deoxy-D-*erythro*-hexos-2-ulose in Aqueous Solution: NMR Evidence of Intramolecular 1,2-Hydrogen Transfer

Wenhui Zhang,[†] Ian Carmichael,[‡] and Anthony S. Serianni*[,†]

[†]Department of Chemistry and Biochemistry, and [‡]Radiation Laboratory, University of Notre Dame, Notre Dame, Indiana 46556, United States

Supporting Information

ABSTRACT: Selective ^{13}C- and ^{2}H-labeling, and ^{13}C NMR spectroscopy, have been used to show that the 1,2-dicarbonyl compound (osone), 3-deoxy-D-*erythro*-hexos-2-ulose (3-deoxy-D-glucosone) (**1**; 3DG), degrades to 3-deoxy-D-*ribo*-hexonic acid **2** and 3-deoxy-D-*arabino*-hexonic acid **3** exclusively via an intramolecular 1,2-hydrogen transfer mechanism in aqueous phosphate buffer at pH 7.5 at 37 °C. Acids **2** and **3** are produced in significantly different amounts (1:6 ratio) despite the prochiral C3 in **1**, and two potential reaction mechanisms are considered to explain the observed stereoselectivity. One mechanism involves acyclic forms of **1** as reactants, whereas the other assumes cyclic pyranose reactants. In the former (2-*keto*-hydrate or 2KH mechanism), putative transition state structures based on density functional theory (DFT) calculations arise from the C1 hydrate form of acyclic **1** having the C1−H1 bond roughly orthogonal to the C2 carbonyl plane. The relative orientation of the alkoxide oxygen atom at C1 and the C2 carbonyl oxygen, and H-bonding between C_1OH and the C2 carbonyl oxygen, contribute to the stability of the transition state. DFT calculations of the natural charges on individual atoms in the transition state show the migrating hydrogen to have an almost neutral charge, implying that it may more closely resemble a hydrogen atom than a hydride anion during transfer from C1 to C2. A second mechanism (2-*keto*-pyranose or 2KP mechanism) involving the cyclic 2-*keto*-pyranoses of **1** as reactants aligns the C1−H1 bond orthogonal to the C2 carbonyl plane in different ring conformations of both anomers, with the β-pyranose giving **3** and the α-pyranose giving **2**. While both the 2KH and 2KP mechanisms are possible, the latter readily leads to a prediction of the reaction stereospecificity that is consistent with the experimental data.

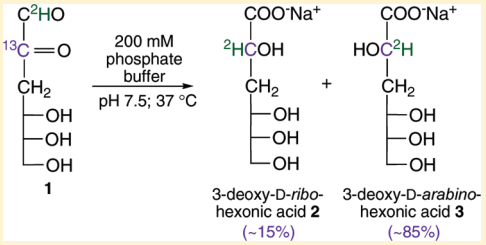

INTRODUCTION

Recent work has shown that the B_6 vitamer, pyridoxamine (PM), can prevent functional damage to proteins by the biologically relevant dicarbonyl compound (osone), 3-deoxy-D-*erythro*-hexos-2-ulose (3-deoxy-D-glucosone) (**1**; 3DG).[1] Efforts to determine the cause of this inhibition led to ^{13}C NMR studies of the solution stability of ^{13}C-labeled 3DG in the presence and absence of PM. These studies showed that **1** degrades slowly in aqueous phosphate buffer at pH 7.5 and 37 °C via two main pathways: skeletal rearrangement (path 1) and backbone oxidative cleavage (path 2) (Scheme 1).[1] In the absence of PM, skeletal rearrangement is favored and produces two C2-epimeric metasaccharinic acids, 3-deoxy-D-*ribo*-hexonic acid **2** and 3-deoxy-D-*arabino*-hexonic acid **3**, in unequal proportions (**2**:**3** = ∼1:6, Scheme 1) after 30 days of reaction. In the presence of PM, oxidative cleavage of the C1−C2 bond is favored, producing formic acid from the terminal C1 of **1**, and the aldonic acid, 2-deoxy-D-*erythro*-pentonic acid (2-deoxy-D-ribonic acid) **4** (Scheme 1) from the remaining carbons. Given the potential importance of these rearrangement reactions *in vivo*, especially in diabetic patients,[1] we decided to investigate path 1 from a mechanistic standpoint.

Prior investigations have shown that aldoses such as D-glucose undergo substantial sketetal rearrangement and/or degradation in aqueous solution upon exposure to alkali.[2−4] Under mildly basic conditions, aldoses isomerize to give mixtures containing the starting aldose, its C2 epimer, and its corresponding 2-ketose (aldose−2-ketose isomerization).[5,6] Under strongly basic conditions, a more extensive sequence of rearrangement reactions ensues, leading initially to saccharinic acids. Studies of the latter reactions with glucose have implicated the presence of **1** along the reaction pathway leading to **2** and **3**, and it has been proposed that this conversion involves a 1,2-hydrogen transfer (benzylic acid rearrangement).[7,8] As discussed by Collins and Ferrier,[9] however, **2** and **3** appear to be produced in approximately equal amounts when D-glucose is treated with aqueous NaOH, and this observation was viewed as consistent with a 1,2-hydrogen transfer mechanism unaffected by asymmetric induction, since C3 is prochiral in 3DG. This induction is observed when D-fructose (or 1-*O*-benzyl-D-fructose) is subjected to similar reaction conditions; in this case, 2-*C*-(methyl)-D-*ribo*-pentonic acid forms almost exclusively.[9] Direct alkaline degradation of **1** has been reported to give different relative amounts of **2** and **3** depending on the nature of the cation used in the reaction (e.g., NaOH vs $Ca(OH)_2$).[10] However, recent work in this laboratory has shown that **1** degrades even under very mild solution conditions (aqueous phosphate

Received: February 7, 2011
Published: July 27, 2011

Scheme 1

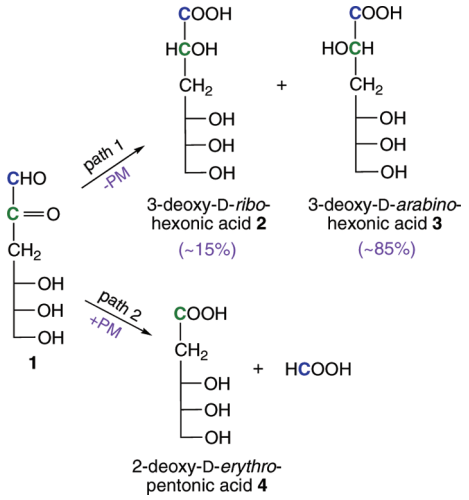

buffer, pH 7.5, 37 °C), and, importantly, gives **2** and **3** in significantly different amounts (~85% **3**; Scheme 1).[1] Under these conditions, 3DG gives products arising mainly from either path 1 (no PM present) or path 2 (with PM present) (Scheme 1), that is, competing degradation pathways that operate under more strongly alkaline conditions appear negligible. Thus, we speculated that the harsher reaction conditions used in prior glucose and 3DG degradation studies may influence the ratio of metasaccharinic acid products because (a) multiple, ill-defined degradation pathways coexist and/or (b) direct base-catalyzed isomerization and/or epimerization of **2** and **3** occurs, thus influencing the final ratio of acids. When these factors are eliminated, the ratio favors one epimer strongly, leading to the question of how this stereoselectivity is achieved without a chiral carbon at C3.

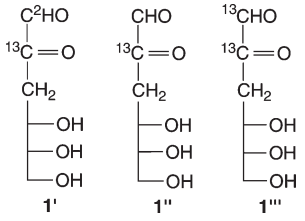

In this report, ^{13}C NMR spectroscopy has been used to investigate the mechanism of conversion of several ^{13}C- and ^{2}H-labeled 3DG substrates (**1**′, **1**″, and **1**‴) to metasaccharinic acids under different solution conditions, and structural factors potentially responsible for the observed reaction stereoselectivity are discussed.

RESULTS AND DISCUSSION

A. ^{13}C NMR Characterization of Skeletal Rearrangement Products from 1′, 1″, and 1‴. In the conversion of osone **1** into metasaccharinic acids **2** and **3**, C1 of the osone is oxidized and C2 is reduced (an internal redox process). To investigate the mechanism of this conversion, the fate of H1 in **1** and the origin of H2 in **2** and **3** were determined using **1** that was selectively deuterated at H1; under these conditions, the detection of ^{2}H at H2 in **2** and **3** provides direct evidence in support of a

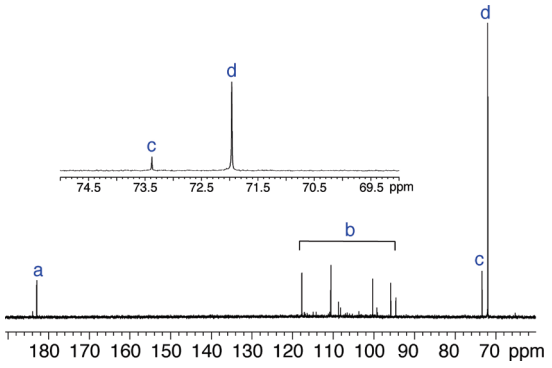

Figure 1. $^{13}C\{^{1}H\}$ NMR spectrum (150 MHz) of a reaction mixture containing [2-^{13}C]3DG (**1**″) in 200 mM phosphate buffer, pH 7.5, after 30 d at 37 °C. Signals "a−d" arise from carbons that are ^{13}C-labeled. Signal "a" is assigned to C1 of **4**, and signals "b" arise primarily from C2 of unreacted **1**″. Signals "c" and "d" (expanded in the inset to show that both signals are singlets) are assigned to C2 of **2** and **3**, respectively.

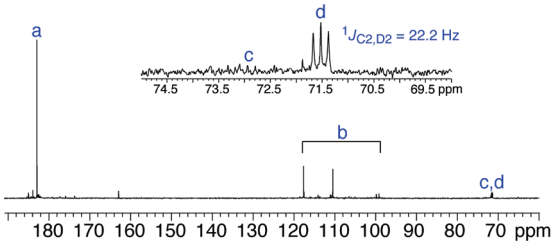

Figure 2. The $^{13}C\{^{1}H\}$ NMR spectrum (150 MHz) of a reaction mixture containing **1**′ in 200 mM phosphate buffer, pH 7.5, after 30 d at 37 °C. Signals "a−d" arise from carbons that are ^{13}C-labeled. Signal "a" is assigned to C1 of **4**, and signals "b" arise partly from C2 of unreacted **1**′. Signals "c" and "d" are assigned to C2 of **2** and **3**, respectively; signal "d" appears as a triplet due to the presence of $^{13}C-^{2}H$ spin-coupling (inset shows the expanded signals "c" and "d" and the measured $^{1}J_{C2,D2}$ in **3**). The triplet from **2** was too weak to detect; its location was inferred from data in Figure 1.

1,2-hydrogen transfer mechanism. In this study, the fate of the deuterium atom was determined by $^{13}C\{^{1}H\}$ NMR spectroscopy using [1-^{2}H; 2-^{13}C]3DG (**1**′) as the reactant. If the ^{2}H attached to C1 of **1**′ is transferred to C2 in **2** and **3** during the reaction, the C2 signals arising from the resulting C2-$^{2}H2$ fragments in the latter should appear as triplets in the $^{13}C\{^{1}H\}$ NMR spectrum. In addition, **1**′ was selectively labeled with ^{13}C at C2 to improve the detection of deuterated C2 carbons in **2** and **3**; sensitivity to detection is lower for C2 in C2-$^{2}H2$ fragments than in C2-$^{1}H2$ fragments because (a) the C2 signals arising from C2-$^{2}H2$ fragments are split by $^{13}C-^{2}H$ scalar coupling, (b) the $^{13}C2$-$^{1}H2$ NOE is absent in C2-$^{2}H2$ fragments, and/or (c) the C2 in C2-$^{2}H2$ fragments relaxes more slowly. In addition, ^{13}C-labeling at C2 improved the overall detection of C2 in **2** and **3** at the moderately low solution concentrations used in this work.

Osone **1**′ (10 mM) was dissolved in 200 mM sodium phosphate buffer, pH 7.5, containing sodium azide (0.2 mg/mL buffer), and the resulting solution was incubated at 37 °C in the dark. $^{13}C\{^{1}H\}$ NMR spectra of the reaction mixture were obtained periodically over the course of 30 days. As a control, [2-^{13}C]3DG (**1**″) was substituted for **1**′ as the reactant in a separate and parallel incubation. Representative $^{13}C\{^{1}H\}$ NMR spectra of these reaction mixtures are shown in Figures 1 and 2.

dx.doi.org/10.1021/jo200288t |J. Org. Chem. 2011, 76, 8151–8158

In the reaction of **1″** (Figure 1), the C2 signals of **2** and **3** appear as singlets with significantly different intensities, confirming a high stereoselectivity favoring **3**.[1,11] In the reaction of **1′** (Figure 2), the C2 signals of **2** and **3** appear as triplets, and the observed $^{1}J_{C2,D2}$ value (~22 Hz) for the predominant acid **3** is consistent with similar couplings observed previously in monodeuterated monosaccharides.[12] C2 signal multiplicity and the observed $^{1}J_{C2,D2}$ value demonstrate that the deuterium attached to C1 of **1′** is transferred to C2 during the conversion of **1′** to **2** and **3**. The weak ^{13}C signal slightly downfield (at ~71.9 ppm) of the triplet assigned to C2 of **3** in Figure 2 is due to a small amount of **3** containing a protonated C2 carbon. This singlet appears downfield of the corresponding deuterated carbon signal due to the ^{2}H isotope effect; the observed shift, δ (^{1}H) − δ (^{2}H), was 53.3 Hz (0.35 ppm) at 150 MHz, in good agreement with 5.3 ± 0.6 Hz shifts reported previously at 15.08 MHz.[12] The C2 carbon in the protonated species should be easier to detect than the C2 carbon in the deuterated species since the former possesses the full $^{13}C2$-$^{1}H2$ NOE and relaxes more rapidly than does the latter, and thus the proportion of protonated form in solution is probably overestimated from a simple integration of the signals. Detection of this protonated species results from the small percentage of ^{1}H attached to C1 of the reactant **1′** (see Figure S1 in Supporting Information for further explanation); its presence does not suggest that a competing non-1,2-hydrogen transfer mechanism is operating.

The effect of solution pH was investigated by conducting a reaction with **1′** in 200 mM sodium phosphate buffer at pH 11.3 and 37 °C, with pH adjusted periodically by manual addition of dilute aqueous NaOH. After 30 days of reaction, the $^{13}C\{^{1}H\}$ NMR spectrum obtained on this reaction mixture was the same as that shown in Figure 2, although time-lapse spectra collected during the course of the reaction showed that the rearrangement occurred at a higher rate at the higher pH. A reaction with **1′** was also conducted at pH 11.3 and 37 °C without sodium phosphate buffer (i.e., in unbuffered aqueous solution); in this case, the initial pH of the reaction mixture was adjusted to 11.3 with NaOH, and the solution pH was maintained by occasional manual additions of dilute aqueous NaOH. $^{13}C\{^{1}H\}$ NMR analyses of this reaction mixture after 30 d showed the formation of **2** and **3** in the same molar ratio as found for reactions conducted in phosphate buffer at pH 7.5 and 11.3, demonstrating that neither the presence of phosphate nor solution pH (neutral to moderately alkaline) influence the mechanism of the reaction and the distribution of C2-epimeric metasaccharinic acids appreciably.

The above findings support the conclusion that the transformation of **1** into **2** and **3** in aqueous phosphate buffer at pH 7.5 and 37 °C occurs exclusively via an internal (intramolecular) 1,2-hydrogen transfer mechanism; competing mechanisms, if they exist, are below the detection limit of these experiments. This transfer dominates over the competing C1−C2 bond cleavage pathway (path 2; Scheme 1) in aqueous phosphate buffer at pH 7.5 and 11.3 and in unbuffered aqueous solution at pH 11.3. 1,2-Hydrogen transfer is accompanied by a strong bias favoring the *arabino*-metasaccharinic acid (**3**), independent of the solution conditions examined. It had been reported previously that both **2** and **3** were produced from D-glucose in similar amounts, and that this observation was consistent with a 1,2-hydrogen transfer mechanism.[9] These prior findings are at odds with the present finding, obtained under relatively mild solution conditions, which shows a conversion that is highly stereoselective yet also involves 1,2-hydrogen transfer.

Scheme 2

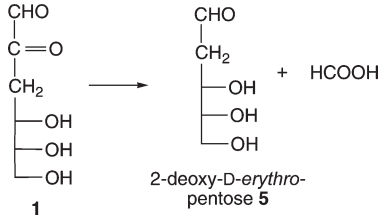

The transfer of hydrogen from C1 of **1** to C2 of products **2** and **3** could also potentially occur via an intermolecular process. This possibility was tested by conducting the rearrangement in sodium phosphate buffer at pH 10.5 and 37 °C using a 1:1 mixture of **1′** and **1‴** as the reactants. In a putative intermolecular mechanism, the H1 atom of **1‴** would be transferred to C2 of **1′**, and the ^{2}H atom at C1 of **1′** would be transferred to C2 of **1‴**. The former process is more easily detected by $^{13}C\{^{1}H\}$NMR, since the signal arising from a protonated C2 carbon in either **2** or **3** would appear as a singlet downfield of the corresponding deuterated C2 carbon, and detection of the former would be favored (see discussion above). $^{13}C\{^{1}H\}$NMR analysis of the reaction mixture showed no significant enhancement of the C2 signal arising from the protonated species above what was detected in Figure 2, thus indicating that the intermolecular process makes a negligible contribution to the rearrangement (see Figure S2 in Supporting Information).

While path 1 dominates in the degradation of **1** in the absence of PM (Scheme 1), ^{13}C NMR analyses of reaction mixtures show that C1−C2 cleavage (path 2; Scheme 1) occurs at a lower level, giving formic acid and **4** as the predominant products (see Figures 1 and 2, and ref 1). This result contrasts with those in a recent report by Brands and van Boekel[13] describing the degradation of D-glucose in 100 mM phosphate buffer, pH 6.8, at 120 °C, presumably via intermediate **1**, involving C1−C2 bond cleavage to give formic acid and the aldopentose, 2-deoxy-D-*erythro*-pentose **5** (Scheme 2). The latter aldopentose was not observed directly in this prior work, but its presence was inferred from the detection of furfuryl alcohol, although the latter was found at levels below that found for HCOOH. In the present study, no evidence for the formation of **5** was obtained regardless of whether PM was present or not in the reaction mixture.

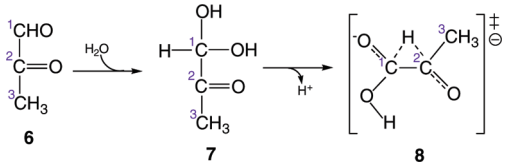

B. Putative Transition States for 1,2-Hydrogen Transfer. The structure of the transition state, and the electronic state of the migrating hydrogen, during 1,2-hydrogen transfer were investigated using density functional theory (DFT) calculations and structure **8** as a model system, which derives from acyclic osone **6** via hemiacetal **7**. In **8**, the migrating hydrogen is partially bonded to both C1 and C2. Conformation about the C1−C2 bond in **7** is important in the formation of **8**. Productive conformations orient the C1−H1 bond roughly orthogonal to the

dx.doi.org/10.1021/jo200288t |*J. Org. Chem.* 2011, 76, 8151–8158

Scheme 3. Bond Lengths (Å) in Transition State A1 from DFT

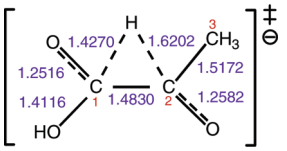

C2 carbonyl plane to allow proper orbital overlap for hydrogen transfer to C2, as shown in structure **9**.

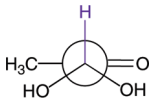

9

Four transition states were investigated (A1, A2, S1, and S2; see Computations) that differ in C1−O1H bond conformation and in configuration at C1. Structure A1 had the lowest energy, followed in increasing energy by S1, A2, and S2, with the latter 6.0 kcal/mol higher in energy than A1. Part of the stabilization of structure A1 is due to the presence of hydrogen bonding between the C_1OH hydrogen and O2 and from partial transfer of that hydrogen from the incipient $C{=}OH^+$ to the incipient carboxylate. Additional structural factors favoring A1 may be the *trans* relationship between the alkoxide anion and the C2 carbonyl oxygen.

DFT calculations provided information on the natural charges of the migrating hydrogen in **8** (Table S1, Supporting Information): −0.007 in A1, −0.016 in A2, −0.018 in S1, and −0.106 in S2. In the lowest energy structure A1, the natural charge on the migrating hydrogen is almost neutral, suggesting that the migrating hydrogen more closely resembles a hydrogen atom than a hydride anion. DFT data for A1 also show that the C1−H and C2−H bond lengths in the transition state differ, with the shorter bond involving C1 (Scheme 3). Similar trends were found in A2, S1, and S2, although the absolute values of the bond lengths varied. From this perspective, the transition state more closely resembles reactant than product. In contrast, the C1−O1$^-$ and C2−O2 bond lengths are very similar in A1, with values intermediate between pure single and double C−O bonds. Similar results were found for A2, but not for S1 and S2. In the latter structures, the C1−O1$^-$ and C2−O2 bond lengths were ∼1.44 Å and ∼1.25 Å, respectively. These results reflect the important effect of C1 configuration on transition state structure. When the oxygens at C1 and C2 are *trans* as found in A1 and A2, similar C−O bond lengths are observed in the transition state, implying greater electronic delocalization. When these atoms are *cis* as found in S1 and S2, less delocalization occurs, and the two bonds differ in length.

C. Structural Factors Affecting the Reaction Stereoselectivity. The Acyclic 2-*keto*-Hydrate (2KH) Mechanism. The present findings support a 1,2-hydrogen transfer mechanism in the conversion of **1** to **2** and **3** under mild solution conditions (pH 7.5, 37 °C). This transformation may involve acyclic forms of **1**, namely, the 1,2-dicarbonyl (**10**) and C1 hydrate (**11**) (Scheme 4). Little is known about the abundances of these and other acyclic forms of **1** in aqueous solution, although recent ^{13}C NMR data on ^{13}C-labeled isotopomers of **1** demonstrate their presence in aqueous solution and suggest abundances lower than 1%.[14] Multiple cyclic forms of **1** predominate in aqueous solution, as reported by Köpper and Freimund.[15]

Scheme 4

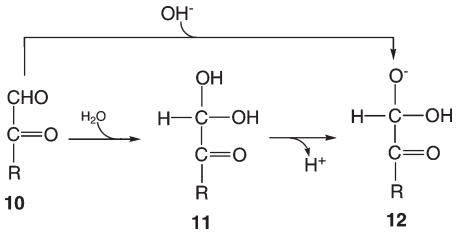

10 **11** **12**

The ionized (alkoxide) form of **11** (**12**; Scheme 4) is a presumed intermediate in the formation of transition state **13**. This form can be generated in two ways: (a) *gem*-diol **11** is deprotonated, or (b) 1,2-dicarbonyl **10** is attacked by hydroxide anion (Scheme 4). Since C1 in **11** is prochiral, the two appended OH groups are diastereotopic, and thus the two OH groups are expected to have different pK_a values. Therefore, at equilibrium, different populations of the two diastereomeric alkoxide anions could contribute to the preferential formation of one of the metasaccharinic acids (see below).

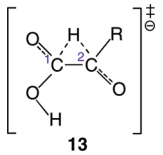

13

At pH 7.5, the metasaccharinic acids **2** and **3** are likely to be fully ionized (deprotonated) in solution (COOH pK_a ∼ 4). This ionization may facilitate 1,2-hydrogen transfer if transition state A1 is involved. In this case, the transfer of H1 from C1 to C2 would be accompanied by O1H proton transfer to O2 (see structure **14**), giving an ionized carboxylate anion and protonated O2 in the products. For this reason, and for those discussed earlier, A1 is considered the most likely transition state for the reaction.

The above arguments can be integrated in a putative acyclic 2-*keto*-hydrate (2KH) reaction mechanism shown in Scheme 5. The A1 transition state is invoked exclusively, with the caveat that other transition states may be involved and thus may exert effects on the reaction stereoselectivity not accounted for here. Ionization of the hemiacetal **11** gives intermediate **I** containing the alkoxide and *keto* oxygens in a *trans* relationship. Subsequent 1,2-hydrogen transfer to the *re* face of the C2 carbonyl occurs in a slow step via transition state **T** to give acid **3**, the major product. Alternatively, rapid C1−C2 bond rotation in **I**, and internal proton transfer, give intermediate **I′** which retains the *trans* relationship between the alkoxide and *keto* oxygens. Subsequent 1,2-hydrogen transfer to the *si* face of the C2 carbonyl via transition state **T′** gives acid **2**, the minor product. The strong stereochemical preference for **3** may be explained by a lower activation barrier to form **T** compared to **T′** (kinetic control) and/or to greater stability of **I** compared to **I′** (thermodynamic control). The stabilities of intermediates **I** and **I′** will be affected by overall molecular conformation but especially by the conformation of the C_4 side chain (R in structures **10**−**13**). If this side chain assumes a pseudocyclic rather than linear-extended conformation, then model inspection shows that it can block the *si* face of the C2 carbonyl sterically from 1,2-hydrogen transfer. Alternatively, side-chain conformation could influence reaction stereoselectivity not by blocking *si* face access to hydrogen transfer but rather by destabilizing the C1−C2 bond conformation

dx.doi.org/10.1021/jo200288t |*J. Org. Chem.* 2011, 76, 8151–8158

Scheme 5

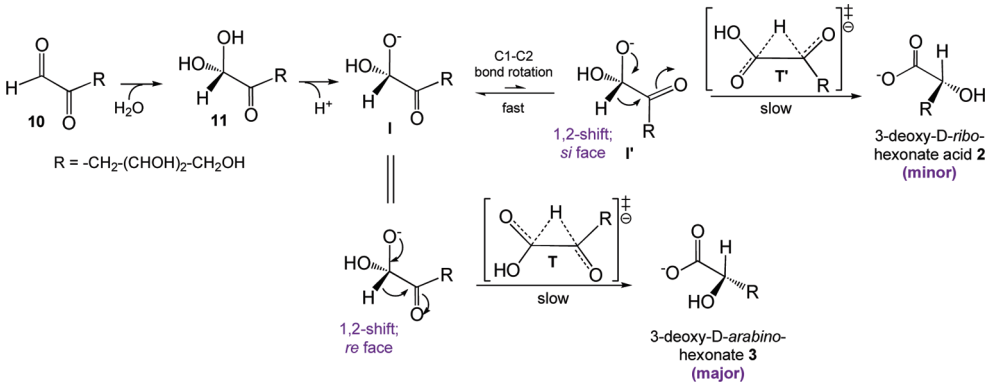

required for *si* face hydrogen transfer. This steric effect would presumably be insufficient to prevent the much smaller hydrogen from transferring to C2 on the *re* face after 180 °C1−C2 bond rotation. Testing these potential models awaits conformational studies of the acyclic C1 hydrate form of **1**.

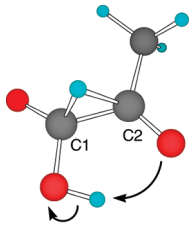

14

D. Cyclic Forms of 1 as Reactive Substrates. The Cyclic 2-*keto*-Pyranose (2KP) Mechanism. Acyclic forms were proposed as the reactive forms of **1** in the above 2KH mechanism (Scheme 5), modeled from previous theoretical studies of related benzylic acid rearrangements of glyoxal and similar substrates.[16] These latter compounds are unable to cyclize, unlike **1**. Thus, consideration should be given to the possibility of cyclic forms of **1** serving as reactive substrates.

NMR analyses[15] of aqueous solutions of **1** have provided the following percentages of monomeric forms at equilibrium: 29% 1,5-pyranose hydrates; 6% 1,4-furanose hydrates; 32% 2,6-pyranose hydrates; 23% 2,5-furanose hydrates; 10% bicyclic forms. The 2-*keto*-pyranose forms **15** and **16**, which could potentially serve as substrates in the rearrangement reaction, are apparently present at the same very low abundances as the acyclic reactants in the 2KH mechanism (Scheme 5). Thus, a 1,2-hydrogen transfer mechanism involving cyclic forms **15** and **16** (2-*keto*-pyranose or 2KP mechanism) is no more or less favored than a mechanism involving acyclic forms based solely on the abundances of reactive species in solution.

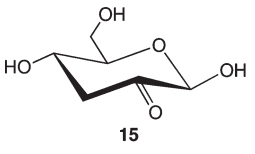

15

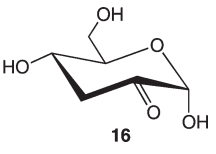

16

Inspection of the two 2-*keto*-pyranoses **15** and **16** shows that both forms can assume a ring conformation that aligns the C1−H1 bond orthogonal to the C2 carbonyl plane, as required from DFT studies of **8** (see structure **9**). In β-pyranose **15**, this alignment is achieved in the $^4C_1$ conformation, whereas in α-pyranose **16**, the pyranose ring must assume a $^1C_4$ form (or related nonchair form) to allow hydrogen transfer to C2. 1,2-Hydrogen migration in the $^4C_1$ form of β-pyranose **15** gives the predominant *manno* product **3**, whereas migration in the $^1C_4$ form of **16** gives the less favored *gluco* product **2**. The initial product generated from hydroxide anion attack on C1 of a 2-*keto*-pyranose reactant is the 1,5-lactone **17** (Scheme 6). $^{13}C\{^1H\}$ NMR analyses of reaction mixtures, however, showed only the presence of aldonate salts as products, although putative intermediate 1,5-lactones might hydrolyze sufficiently fast at pH 7.5 and 37 °C to elude detection.[17,18] The transition states for the pyranose reactants are structurally related to the higher-energy *syn* isomers S1 and S2 that are not stabilized by H-bonding. An effort was made to model the transition state shown in Scheme 6 by DFT, as was done for **8**. However, these calculations failed to yield a reliable transition state structure; instead, geometry optimization led to spontaneous anomerization of **15** into a 2,5-furanose form of **1** containing an exocyclic aldehydic moiety.

An alternative cyclic mechanism for the reaction might also involve 2-*keto*-furanoses such as **18** and **19**. A 2-*keto*-furanose (2KF) mechanism would presumably involve the E_1 conformation of **18** and the ^1E conformation of **19** in which proper alignments of the C1−H1 bond with respect to the C2 carbonyl plane are achieved. Unlike the 2KP model, however, the 2KF model does not lead to a clear prediction of the reaction stereospecificity.

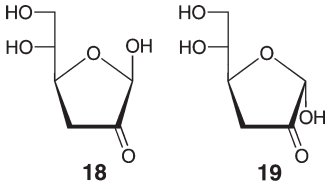

18 **19**

In summary, a mechanism invoking cyclic forms of **1** as the reactive forms can explain the observed stereochemistry of the reaction if 1,2-hydrogen transfer occurs in **15** more rapidly than in **16**. The latter assumption appears reasonable based on the need for **16** to assume a presumably higher-energy ring conformation to promote hydrogen transfer. The relative abundances of **15** and **16** in solution, while currently unknown, may also influence the reaction stereochemistry.

dx.doi.org/10.1021/jo200288t |*J. Org. Chem.* 2011, 76, 8151–8158

Scheme 6

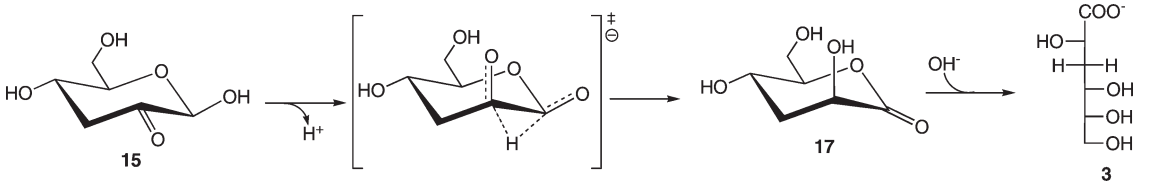

CONCLUSIONS

Selective ^{13}C- and ^{2}H-labeling has been used to show that 3DG rearrangement in aqueous phosphate buffer at pH 7.5 at 37 °C to give metasaccharinic acids **2** and **3** occurs exclusively via an intermolecular 1,2-hydrogen transfer mechanism. Two reaction mechanisms were considered, one involving the acyclic 2-*keto*-hydrate form of **1** as the reactant (2KH mechanism), and the other involving the 2-*keto*-pyranoses (2KP mechanism). In the former, which mimics the reaction pathways posited for 1,2-dicarbonyl compounds such as glyoxal, putative transition states based on density functional theory (DFT) calculations orient the C1−H1 bond roughly orthogonal to the C2 carbonyl plane to promote hydrogen transfer. The relative orientation of the alkoxide oxygen at C1 and the C2 carbonyl oxygen, and H-bonding between C_1OH and the C2 carbonyl oxygen, appear to influence the stability of the transition state. Calculations of the natural charges on individual atoms in the transition state show the migrating hydrogen to have an almost neutral charge, implying that it may more closely resemble a hydrogen atom than a hydride anion during transfer. In the 2KP mechanism, the 2-*keto*-pyranose forms of **1** serve as reactants, with both anomers allowing a similar relative disposition of the C1−H1 bond and C2 carbonyl plane in the transition state as found in the 2KH mechanism. For the β-anomer, this geometry is achieved in the $^{4}C_1$ (or related) ring conformation, whereas in the α-anomer, a $^{1}C_4$ (or related) conformation is required. Minor forms of **1** in solution are implicated as the reactive forms in both mechanisms.

Metasaccharinic acids **2** and **3** are produced in significantly different amounts under mild solution conditions despite the prochiral C3 adjacent to the reaction centers at C1 and C2 of **1**. An analysis of the structural features of putative intermediates and transition states of the 2KH mechanism suggests that overall conformation of the C1 hydrate form of **1** may play a key role in determining the relative susceptibilities of the *re* and *si* faces of the C2 carbonyl to 1,2-hydrogen transfer. Two modes of stereochemical control were identified. In the first, the C_4 side chain blocks one face of the C2 carbonyl. In the second, the side chain controls the reaction stereoselectivity by influencing C1−C2 bond conformation. While these conformational factors may exist, they are difficult to quantify experimentally and computationally. In contrast, a more satisfying argument for the reaction stereoselectivity emerges from the 2KP mechanism. In this case, the β-pyranose, which presumably assumes a relatively low-energy reactive conformation ($^{4}C_1$) in solution, rearranges to give the more favored *manno* product **3**, whereas the α-anomer, which presumably must assume a higher-energy reactive conformation ($^{1}C_4$), rearranges to give the less favored *gluco* product **2**. The comparatively direct explanation of the observed reaction stereoselectivity afforded by the 2KP mechanism is a key factor favoring this mechanism over the 2KH mechanism.

The mechanistic findings described herein for the rearrangement of **1** lead to the question of whether its well-known analogue, D-glucosone (D-*arabino*-hexos-2-ulose) **20**, experiences a similar rearrangement in solution involving 1,2-hydrogen transfer. Interestingly, recent NMR studies of ^{13}C-labeled **20** under solution conditions similar to those used for the present 3DG work reveal significantly different reactivity. These results point to the important role of O3 adjacent to the C2 carbonyl in directing the rearrangement and degradation of 1,2-dicarbonyl sugars. The results of NMR studies of **20** will be discussed in an upcoming report.

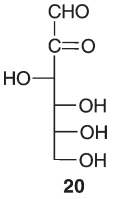

EXPERIMENTAL SECTION

A. Synthesis of $^{13}C/^{2}H$-Labeled 3-Deoxy-D-erythro-hexos-2-uloses 1. D-[1-^{2}H; 2-^{13}C]3DG (**1′**), D-[2-^{13}C]3DG (**1″**), and D-[1,2-$^{13}C_2$]3DG (**1‴**), were prepared from 3-deoxy-D-[1-^{2}H;2-^{13}C]-*ribo*-hexopyranose, 3-deoxy-D-[2-^{13}C]*ribo*-hexopyranose, and 3-deoxy-D-[1,2-$^{13}C_2$]*ribo*-hexopyranose, respectively, as described previously.[1] 3-Deoxy-D-[1-^{2}H;2-^{13}C]*ribo*-hexopyranose, 3-deoxy-D-[2-^{13}C]*ribo*-hexopyranose, and 3-deoxy-D-[1,2-$^{13}C_2$]*ribo*-hexopyranose were obtained from Omicron Biochemicals, Inc. (South Bend, IN).

B. NMR Spectroscopy. $^{13}C\{^{1}H\}$ NMR spectra of reaction mixtures were obtained on 90% H_2O/10% $^{2}H_2O$ (*v*/*v*) solutions (aliquots were withdrawn from reaction mixtures and diluted with $^{2}H_2O$ prior to analysis) at 30 °C. Samples were analyzed in 3-mm NMR tubes on a FT-NMR spectrometer operating at 150.854 MHz for ^{13}C and equipped with a 3-mm dual $^{13}C/^{1}H$ microprobe. ^{13}C Chemical shifts were referenced externally to sodium 4,4-dimethyl-4-silapentane-1-sulfonate (DSS). $^{13}C\{^{1}H\}$ NMR spectra were collected with ∼37 000 Hz spectral windows and ∼4.0 s recycle times. FIDs were processed to optimize spectral S/N (exponential line-broadening = 1 Hz) and final spectra had digital resolutions of ∼0.14 Hz/pt.

COMPUTATIONS

All calculations were conducted using *Gaussian*09.[19] The 1,2-hydrogen transfer reaction mechanism was modeled using structure **21**, which is the putative intermediate representing the ionized C1 hydrate form of **1**, and transition states A1, A2, S1, and S2 (Scheme 7) that link **21** to end-products **22** and **23**; the latter are structural analogues of **2** and **3**, respectively. Structures A1 and A2 orient the alkoxide oxygen at C1 and the oxygen atom at C2 *anti* ($O1_{alkoxide}$−C1−C2−O2 torsions of −159° and −158°, respectively), and structures S1 and S2 orient these two atoms *syn*

dx.doi.org/10.1021/jo200288t |*J. Org. Chem.* 2011, 76, 8151–8158

Scheme 7

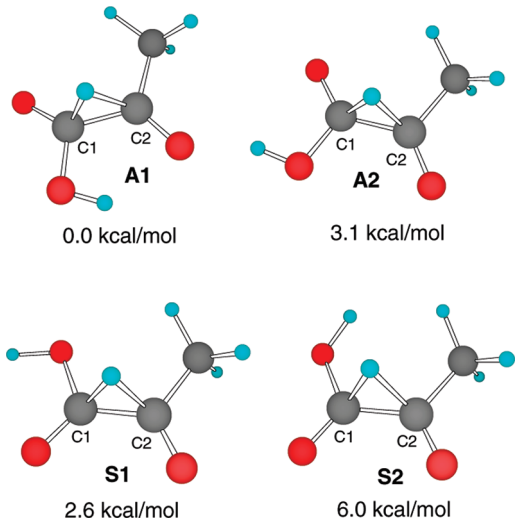

($O1_{alkoxide}$−C1−C2−O2 torsions of 1° and −4°, respectively). Structures A1 and A2 differ in the C2−C1−O1−H torsion angle (2° and −177°, respectively), and structures S1 and S2 have corresponding torsion angles of −177° and −39°, respectively. Structures of **21** and the four transition states were obtained from density function theory (DFT) calculations using the B3LYP functional[20] and the polarized split-valence basis set, 6-31G*.[21] Geometries were fully optimized using analytic gradients, and the various stationary points obtained were characterized from the corresponding analytic Hessians. Energetics were refined using the same functional with the more flexible 6-311+G(d,p) basis set.[22] Relative energies in solution were estimated after reoptimizing the structures in the presence of a solvent field using the recently improved IEFPCM approach.[23] Natural atomic charges were computed using this same basis set and the NBO module[24] available within the *Gaussian*09 suite.

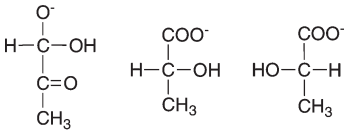

■ ASSOCIATED CONTENT

Supporting Information. ^{1}HNMR analyses of ^{13}C and ^{2}H-enrichment in the chemical precursor used to prepare 3-deoxy-D-[1-^{2}H;2-^{13}C]*erythro*-hexos-2-ulose **1′** (Figure S1); $^{13}C\{^{1}H\}$ NMR studies of potential intermolecular hydrogen transfer using mixed isotopomers of **1** (Figure S2); natural charges on atoms in transition state structures A1, A2, S1, and S2 calculated by DFT (Table S1); Cartesian coordinates of transition state structures A1, A2, S1, and S2 from DFT calculations (Table S2); complete ref 19. This material is available free of charge via the Internet at http://pubs.acs.org.

■ AUTHOR INFORMATION

Corresponding Author
*E-mail: aseriann@nd.edu.

■ ACKNOWLEDGMENT

This work was supported by the National Institute of Diabetes and Digestive and Kidney Disease (DK065138). A.S. thanks Omicron Biochemicals, Inc. (South Bend, IN), for the generous gifts of 3-deoxy-D-[1-^{2}H;2-^{13}C]*ribo*-hexopyranose, 3-deoxy-D-[2-^{13}C]*ribo*-hexopyranose, and 3-deoxy-D-[1,2-$^{13}C_2$]-*ribo*-hexopyranose. The authors thank Prof. Charles Perrin for suggesting the possibility of a 2KP mechanism. The Notre Dame Radiation Laboratory is supported by the Office of Basic Energy Sciences of the United States Department of Energy. This is Document No. NDRL-4877 from the Notre Dame Radiation Laboratory.

■ REFERENCES

(1) Chetyrkin, S. V.; Zhang, W.; Hudson, B. G.; Serianni, A. S.; Voziyan, P. A. *Biochemistry* **2008**, *47* (3), 997–1006.
(2) Hough, L.; Richardson, A. C. The Monosaccharides: Pentoses, Hexoses, Heptoses and Higher Sugars. In *Rodd's Chemistry of Carbon Compounds*; Coffey, S., Ed.; Elsevier: Amsterdam, 1967; Vol. 1F, pp 251−262.
(3) Isbell, H. S. Enolization and Oxidation Reactions of Reducing Sugars. In *Advances in Chemistry Series*; Gould, R. F., Ed.; Carbohydrates in Solution; American Chemical Society: Washington, DC, 1973; 117, pp 70−87.
(4) Speck, J. C., Jr. *Adv. Carbohydr. Chem.* **1958**, *13*, 63–103.
(5) Lobry De Bruyn, C. A.; van Ekenstein, W. A. *Recl. Trav. Chim. Pays-Bas* **1895**, *14*, 203–216.
(6) King-Morris, M. J.; Serianni, A. S. *Carbohydr. Res.* **1986**, *154*, 29–36.
(7) Nef, J. U. *Ann.* **1910**, *376*, 1.
(8) Anet, E. F. L. J. *Adv. Carbohydr. Chem.* **1964**, *19*, 181–218.
(9) Collins, P. M.; Ferrier, R. J. *Monosaccharides: Their Chemistry and Their Roles in Natural Products*; Wiley: New York, 1995; pp 139−144.
(10) Machell, G.; Richards, G. N. *J. Chem. Soc.* **1960**, 1938–1944.
(11) The assignment of the predominant acid produced from **1** was made by preparing authentic sodium 3-deoxy-D-*ribo*-hexonate (sodium 3-deoxy-D-gluconate) and comparing its $^{13}C\{^{1}H\}$ NMR spectrum with those obtained on 3DG reaction mixtures under the same solution conditions (phosphate buffer, pH 7.5, 30 °C).[1] The signals in the standard spectrum matched those arising from the less abundant isomer in the 3DG reaction mixtures.
(12) Serianni, A. S.; Barker, R. *Can. J. Chem.* **1979**, *57*, 3160–3167.
(13) Brands, C. M.; van Boekel, M. A. J. S. *J. Agric. Food Chem.* **2001**, *49*, 4667–4675.
(14) Zhang, W.; Serianni, A. S. Unpublished results.
(15) Köpper, S.; Freimund, S. *Helv. Chim. Acta* **2003**, *86*, 827–843.
(16) Rajyaguru, I.; Rzepa, H. S. *J. Chem. Soc., Perkin Trans 2* **1987**, 1819–1827.
(17) We did not attempt to prepare the lactones of **2** and **3** to test their rates of hydrolysis at pH 7.5 and 37 °C since cyclization of the acyclic aldonic acids is likely to give both 1,4- and 1,5-lactones, with presumably the former more highly favored.
(18) Lactonization of D-mannonic acid favors the formation of the 1,4- lactone, and 1,4-cyclization is likely to be even more favored than 1,5-cyclization for **3**. It is possible that the less stable 1,5-lactone hydrolyzes more rapidly in solution than the 1,4-lactone, thus explaining the failure to detect its presence in the reaction mixture. While lactonization of D-gluconic acid favors the 1,5-lactone over the 1,4-lactone, hydrolysis of the former may still be sufficiently rapid at pH 7.5 and 37 °C to avoid detection.
(19) Frisch, M. J., et al. *Gaussian09, Revision A.1*, Gaussian, Inc., Wallingford, CT, 2009.
(20) Becke, A. D. *J. Chem. Phys.* **1993**, *98*, 5648–5652.
(21) Hehre, W. J.; Ditchfield, R.; Pople, J. A. *J. Chem. Phys.* **1972**, *56*, 2257–2261.

(22) Frisch, M. J.; Pople, J. A.; Binkley, J. S. *J. Chem. Phys.* **1984**, *80*, 3265–3269.
(23) Scalmani, G.; Frisch, M. J. *J. Chem. Phys.* **2010**, *132*, 114110–114115.
(24) Glendening, E. D.; Reed, A. E.; Carpenter, J. E.; Weinhold, F. *NBO Version 3.1*.